

PROMOTED PLATINUM DEHYDROGENATION CATALYST ON A NANO- SIZED GAMMA ALUMINA SUPPORT

Mandana Akia^{1,2,3*}, Seyed Mahdi Alavi¹, Zi-Feng Yan³

¹Chemical Engineering Department, Iran University of Science and Technology, Tehran, Iran, ²Chemical Engineering Department, Kermanshah University of Technology, Kermanshah, Iran, ³State Key Laboratory for Heavy Oil Processing, Key Laboratory of Catalysis, CNPC, China University of Petroleum, Dongying 257061, China

Received September 9, 2010, Accepted October 15, 2010

Abstract

In this paper, a high surface area nanocrystalline gamma alumina has been synthesized with the sol-gel method. The effects of different platinum loadings on the activity of Pt-based dehydrogenation catalyst were investigated. The prepared samples were characterized by X-ray diffraction (XRD), N₂ adsorption (BET), Transmission electron microscopy (TEM), Scanning electron microscopy (SEM), Inductive coupled plasma atomic emission spectroscopy (ICP-AES), Temperature programmed reduction (TPR) and CO chemisorptions techniques. The catalytic results demonstrated very high selectivity relative to monoolefin formation at different reaction temperatures for all the samples prepared. The results revealed that the conversion did not increase by increasing the platinum loading. Comparing the catalytic results of sample DH-2 (0.2 wt% of Pt) with a commercial catalyst (0.4 wt% of Pt), it is noticed that the catalysts prepared with the synthesized nanocrystalline gamma alumina support performed well as an efficient catalyst for dehydrogenation of higher normal paraffins (C₁₀-C₁₅).

Keywords: Nanomaterials; Sol-gel preparation; γ -Al₂O₃; Dehydrogenation catalyst; Higher normal paraffins.

1. Introduction

Dehydrogenation of hydrocarbons is an important commercial process because of the great and expanding demand for dehydrogenated hydrocarbons for use in the manufacture of various chemical products [1]. All the dehydrogenation catalysts of long chain paraffins are designed to produce linear olefins for the manufacture of biodegradable detergents from raw materials such as C₁₀ to C₁₃, C₁₁ to C₁₄ and C₁₁ to C₁₅ [2].

The first announcement of the successful catalytic dehydrogenation process was made in 1935. Chromia-alumina catalysts were originally employed for the dehydrogenation of light hydrocarbons (e.g., n-C₂, C₃, C₄ and i-C₄). In the 1960s a different approach with noble metal (Pt) catalysts to catalytic dehydrogenation was introduced for the first time to supply the long chain linear olefins for the production of biodegradable detergents [3].

Platinum and platinum-containing bimetallic catalysts supported on alumina are widely used for naphtha reforming and for heavy linear paraffins dehydrogenation in the petrochemical industries [4-5]. The dehydrogenation catalyst rapidly deactivates due to fouling by heavy carbonaceous materials. Therefore, the properties of platinum and the alumina support need to be modified to suppress the formation of by-products and to increase catalytic stability [2, 6-8]. The key role of dehydrogenation catalysts is to accelerate the main reaction while controlling the other side reactions [8].

In dehydrogenation of long chain alkanes, a multimetallic alumina supported platinum catalyst is implemented, which contains In and Sn promoters as platinum modifiers, and alkaline and alkaline-earth metals as support modifiers [9-10].

The addition of Sn to Pt/Al₂O₃ catalysts improves the activity and selectivity to olefins, while increasing the catalyst stability in higher normal paraffins dehydrogenation [11-13]. Indium as a modifier decreases the hydrogenating capacity of alumina and suppresses olefin cracking and isomerization, probably as a result of a decrease in the acidic function of the support [14-15]. Incorporation of iron in this catalyst increases both the activity and the stability of the catalyst [6, 9]. The improvement of the catalytic properties of platinum by using modifiers are explained by two effects including a variation of the bond strength between chemisorbed hydrocarbons or intermediates and the surface atoms because of the interaction between the two metals (ligand effect) and a dilution of platinum ensembles by the second metal (ensemble effect) [16].

Alumina is the most widely used support material for the dehydrogenation catalysts because of its superior capability to maintain a high degree of platinum dispersion which is essential for achieving high dehydrogenation activity. But its strong acidity causes side reactions and coke formation [8]. The addition of alkaline and alkaline-earth ions (e.g. Li) to γ -Al₂O₃ selectively would poison the isomerization active sites, with no effect on the dehydrogenation capacity of the catalytic systems [17]. In general the effect of support promoters might be explained as modifying the metal dispersion, blocking the acidic sites of the supports, promoting the hydrogen spillover, diminishing the amount of coke formed on the catalysts (not only the supports, but also the active metal sites) and increasing the fraction of bare metallic Pt surface after carbon deposition [3].

The sol-gel techniques have been widely applied for the synthesis of highly porous alumina which was originally developed by Yoldas [18]. The advantages of the sol-gel method includes the ability of maintaining high purity, changing the physical characteristics such as pore size distribution, pore volume and preparing samples at low temperatures [19-20].

The majority of multicomponent catalysts for the dehydrogenation of higher normal paraffins have been reported in patents [9-10] and there are few research paper in this field [3]. In this study, a high surface area nanocrystalline gamma alumina support was synthesized by the sol-gel method and employed as a catalyst carrier for higher normal paraffins (C₁₀-C₁₅) dehydrogenation catalyst (Pt-based catalyst).

2. Experimental

2.1. Materials

The starting materials for support preparation were aluminium isopropoxide, (AIP, 99 wt%), hexadecyl trimethylammonium bromide (C₁₆TMABr, 99 wt%), and nitric acid. For catalyst composite hexachloroplatinic acid (H₂PtCl₆), tin chloride (SnCl₂), indium chloride (InCl₃), lithium nitrate (LiNO₃), iron nitrate (Fe(NO₃)₃) and hydrochloric acid (HCl) were used. Hexachloroplatinic was purchased from Riedel Co. and the other materials were purchased from Merck Co. and used as received without further purification. The commercial dehydrogenation catalyst (DP-805) was provided from the French Company IFP.

2.2. Support preparation

The nanocrystalline gamma alumina was prepared using the method described [21-22]. In short, aluminium isopropoxide and hexadecyltrimethyl ammonium bromide were first dissolved in water. The molar ratios of water to AIP and hexadecyltrimethyl ammonium bromide to AIP were chosen as 80 and 0.8, respectively. The hydrolysis step was carried out at a temperature of 80°C for a time period of 30 min, under vigorous stirring. Subsequently the mixture was peptized using nitric acid (10 wt.%) under vigorous stirring by careful pH adjustment to 4.5. The mixture was aged at ambient temperature for 5 h. The condensation of the mixture resulted from the evaporation of the solvent by heating the reaction mixture and subsequent drying in an oven at 110°C for 15 h. Finally, the dried sample was calcined at 600°C for 5h in order to remove the surfactant and obtain the gamma crystallite phase.

2.3. Catalyst preparation

The dehydrogenation catalyst consists of a synthesized gamma alumina support which contains 0.5 wt.% of tin, 0.3 wt.% of indium, 0.2 wt.% Fe, 0.6 wt.% of lithium and less than 0.1 wt.% of chloride with various platinum weight percentages of 0.1, 0.2, 0.3, 0.4 and 0.5 wt.%. The effects of promoters loadings and their optimization is being considered in a work

in progress by M. Akia et al. The catalysts were prepared by the wet impregnation method. In a typical preparation method, Sn, In and Fe were first co-impregnated on the gamma alumina support in a solution containing SnCl_2 , $\text{In}(\text{Cl})_3$, $\text{Fe}(\text{NO}_3)_3$ and 10 wt.% HCl. This mixture was aged at the room temperature for 4 h under stirring conditions. Then it was dried at 80 °C for 18 h in a vacuum oven and calcined at 540 °C for 2 h in an atmosphere of air. In the second step, the dried sample was impregnated in an aqueous solution containing a mixture of H_2PtCl_6 and 10 wt.% HCl to obtain the desired content of platinum followed by aging and drying as described. To reduce its chloride content to 0.1 wt%, this is responsible for the side reactions, wet calcination was performed at a mixture of air and water (1:1 molar ratio). The resultant sample was further calcined in air atmosphere at 500 °C for 2 h. In the final step, the dehalogenated sample was impregnated with an aqueous solution of $\text{LiNO}_3/\text{HNO}_3$, followed by drying and calcination as described earlier. All the catalysts were prepared with the same procedure with the changes in the platinum loading which named DH samples. Analysis of the final catalyst samples have been carried out by the inductive coupled plasma (ICP) technique. The actual concentrations determined by the ICP–AES analyses were in good agreement with the theoretical values.

2.4. Characterization

To examine the crystallinity of the prepared samples, powder X-ray diffraction (XRD) analysis was carried out with a MAC Science Co. M18XHF diffractometer using $\text{CuK}\alpha$ X-ray radiation ($\lambda = 0.1540$ nm). The surface area (BET), pore size distribution and pore volume were determined by nitrogen adsorption at -196°C using an automated gas adsorption analyzer (Tristar 3000, Micromeritics). Transmission Electron Microscopy (TEM) investigation was performed with JEOL JEM-2100UHR operated at 200 Kv. Scanning Electron Microscopy (SEM) was performed with HITACHI S-4800 FE-SEM operated at 5 kV. Inductive Coupled Plasma Atomic Emission Spectroscopy (ICP–AES) was performed in a Shimadzu (Japan) ICPV-1000 apparatus. Temperature Programmed Reduction (TPR) was carried out using an automatic apparatus (ChemBET-3000 Quantachrome) equipped with a thermal conductivity detector. The fresh catalyst (500 mg) was subjected to a heat treatment ($10^\circ\text{C}/\text{min}$) in a gas flow (50 ml/min) containing a mixture of H_2 : Ar (10:90). Before conducting the TPR experiment, the sample was heat treated under an inert atmosphere at 400 °C for 3 h. Infrared spectra for CO chemisorptions were recorded on a NEXus fourier transform infrared (FTIR) spectrophotometer.

2.5. Experimental set-up and feed compositions for catalysts evaluation

Major sections of the experimental set-up used for the catalyst evaluation are: hydrogen flow control module, liquid pumping system, preheater and mixer, reactor, condenser and gas–liquid separator, adequate flow meters to account material balance. The reactor is a tubular fixed bed type with an inner diameter of 8 mm which is operated in isothermal and down-flow mode. Reactor internal temperature is measured with a central temperature probe with 3 thermocouples. Reactor inlet pressure is continuously monitored with a pressure transmitter, Figure 1.

Prior to the experiments all the catalysts, previously 20-40 mesh sieved, were reduced under flowing H_2 at 430°C for 4 h with a heating rate of $5^\circ\text{C}/\text{min}$. These catalysts were tested for 18 h on stream. The dehydrogenation reactions were carried out at three temperatures; 460, 475 and 490°C . The reactor effluent is first cooled down in a water cooler before entering separator. Liquid analysis is performed on the product for analysis of the following components: Paraffins, olefins and diolefins, iso-paraffins, alkyl aromatics and alkyl naphthenes and cracked products. This is achieved with the FID detector and the HP PONA column.

The reaction conditions and feed compositions have been summarized in Tables 1 and 2, respectively. In this reaction hydrogen is utilized in amounts sufficient to insure hydrogen to hydrocarbon mole ratio of about 6:1. Excess hydrogen is necessary in the dehydrogenation of lower and higher paraffins. Hydrogen serves as a dual-function in both diluting the paraffin and suppressing the formation of hydrogen deficient, carbonaceous deposits on the catalyst composite [8, 11].

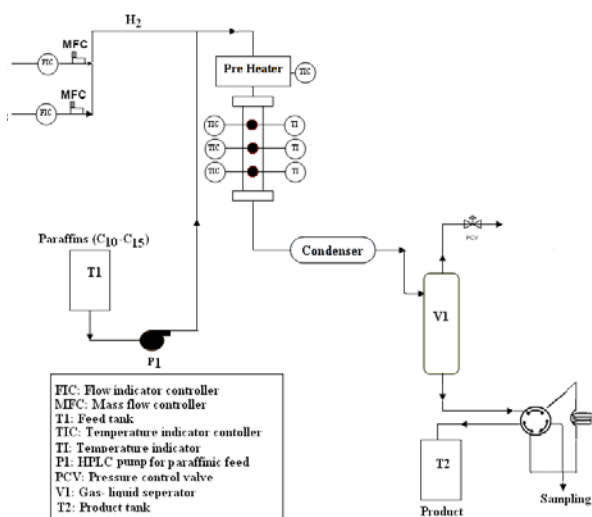


Fig. 1. The schematic of the set-up for the dehydrogenation of higher normal paraffins

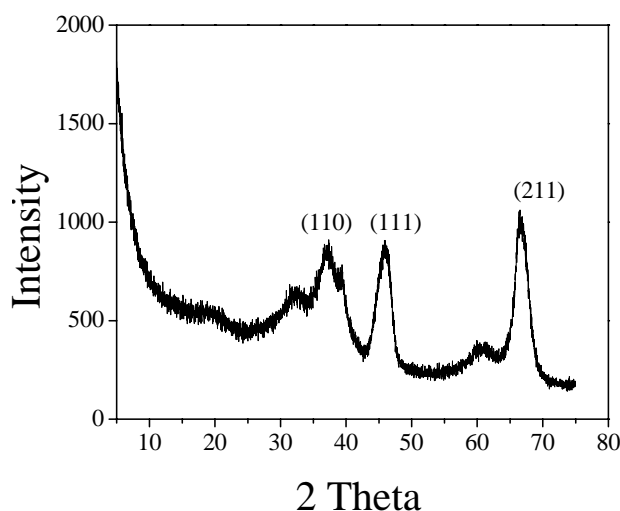


Fig. 2. XRD pattern of the prepared support calcined at 600°C

Table 1. The operating parameters in the dehydrogenation of higher normal paraffins

Feed	Operating parameters	Reactor type
Normal paraffins (C ₁₀ -C ₁₅) Hydrogen (with 99.99% purity)	Temperature: 460-490°C Pressure: 1.7 bar Liquid hourly space velocity (LHSV) of feed: 20 h ⁻¹ , Hydrogen/hydrocarbon molar ratio: 6	Down- flow fixed bed reactor

Table 2. Higher paraffins composition as the feed for dehydrogenation reaction

Component	wt. %	Component	wt. %
N-C9	0.15	N-C15	2.67
N-C10	7.16	N-C16	0.63
N-C11	25.78	N-C17	0.1
N-C12	29.46	N-C18	0.02
N-C13	24.05	N-C19	0.007
N-C14	7.18	Total non normal	2.793

3. Results and discussion

3.1 Texture and surface properties of γ -alumina support

Aluminum alkoxide is hydrolyzed with water, producing either aluminum mono- or tri-hydroxides. In both cases the X-ray diffraction patterns of the initial products are not different. Poorly crystallized boehmite ('pseudoboehmite') develops after a few hours as the precipitate is being aged. Boehmite is the only phase which occurs when the temperature exceeds 77°C during the hydrolysis reaction or during aging of an initially amorphous precipitate [22-23]. The XRD pattern of the alumina sample calcined at 600°C is shown in Figure 2. As it can be seen, the sample is in the gamma crystallite phase.

The nitrogen adsorption/desorption isotherm and pore size distribution of the Al₂O₃ calcined at 600°C are shown in Figure 3. It can be concluded that the sample exhibits the classical shape of a type IV isotherm according to the IUPAC classification, typical for mesoporous solids [24]. However, for this sample, a hysteresis loop (type H1) occurs at a higher relative pressure range ($p/p_0 = 0.7-0.9$) suggesting a broad pore size distribution with a uniform size and shape. The pore size distribution (Figure 3, upper inset) indicates a mesoporous structure and also confirms a relatively broad pore size distribution. The BET surface area, average

pore diameter and pore volume for the synthesized support were $242.9 \text{ (m}^2\text{g}^{-1}\text{)}$, 16.5 (nm) and $1.42 \text{ (cm}^3\text{g}^{-1}\text{)}$, respectively.

Figure 4 shows the SEM image of the synthesized nanocrystalline gamma alumina. The SEM result indicates some agglomeration on the surface. Figure 5 shows the TEM and the high-resolution images of the synthesized nanocrystalline gamma alumina. As it can be seen the prepared alumina highly crystallized with almost uniform size and/or shape particles. The TEM images indicate the presence of hexagonal crystal structure. The results confirm the nanocrystallinity of the synthesized gamma alumina support (less than 4 nm).

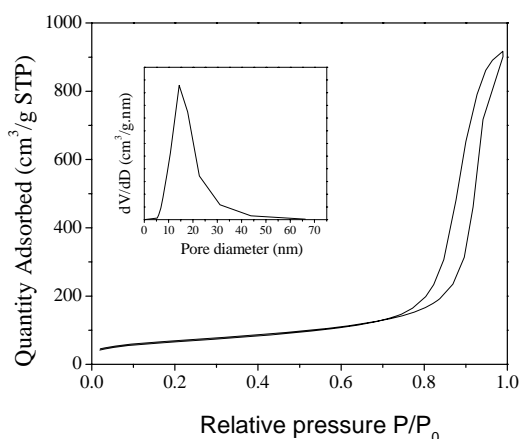


Fig. 3. Nitrogen adsorption/desorption isotherm and pore size distribution (upper inset) of the gamma alumina support calcined at 600°C

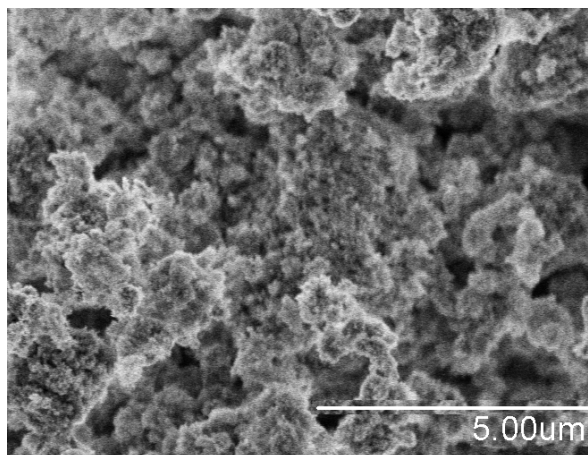


Fig. 4. The SEM micrograph of gamma alumina prepared by the sol-gel method

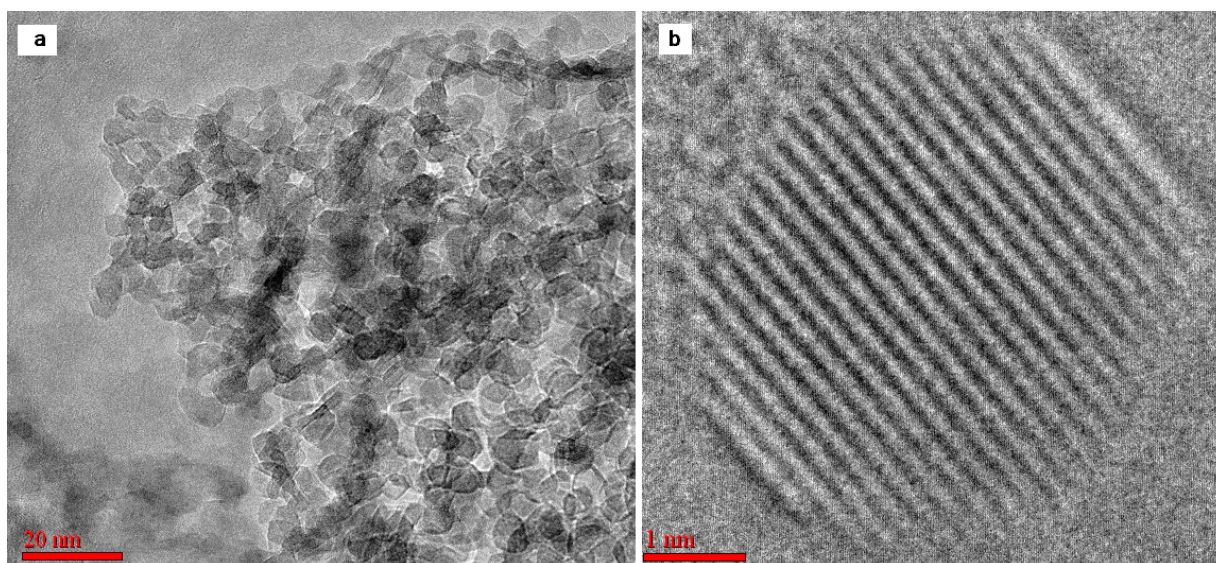


Figure 5. (a) TEM image of the prepared $\gamma\text{-Al}_2\text{O}_3$ sample calcined at 600°C and (b) high-resolution image of gamma alumina nano particles

3.2 Catalyst characterization

3.2. 1 Textural properties of the prepared catalysts

The textural properties of the prepared catalyst samples have been presented in Table 3. The actual concentration of platinum corroborated by ICP can be seen in Table 3.

The BET surface area decreases while the platinum loading increases. The average pore diameter and pore volume of all the prepared catalysts were quite near. These results indicate that metals impregnation occlude a proportion of mesopores in the support.

Figure 6 shows the nitrogen adsorption isotherms at -196°C and the BJH pore size distributions (upper inset) of the catalysts prepared. The isotherms show the classical shape of the type IV according to the IUPAC classification, exhibiting H1 hysteresis loops, typical for mesoporous solids [24].

Table 3. Textural properties of the prepared catalysts with different platinum contents

Sample	Platinum content (wt %)	BET area (m^2g^{-1})	Average pore diameter (nm)	Pore volume (cm^3g^{-1})
DH-1	0.11	186.59	7.24	0.50
DH-2	0.21	184.39	7.27	0.49
DH-3	0.32	182.63	7.40	0.50
DH-4	0.41	168.32	7.54	0.45
DH-5	0.52	165.81	7.60	0.46

The pore size distributions of the samples prepared with different platinum loadings are presented in Figure 7. As it can be seen, all the samples show narrow pore size distributions.

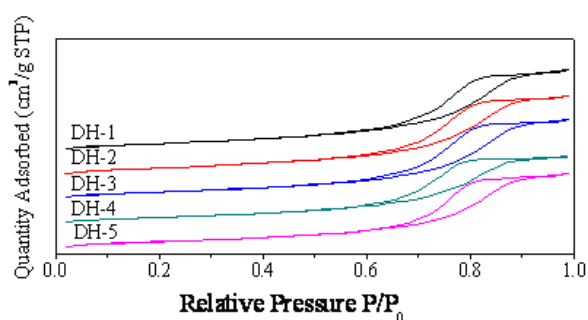


Fig. 6. Nitrogen adsorption/desorption isotherm of the prepared catalysts with different platinum contents

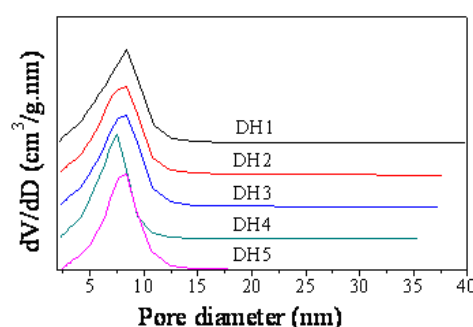


Fig. 7. Pore size distribution of the samples prepared with various platinum loadings

3.2.2 Temperature programmed reduction (TPR)

Figure 8 shows the TPR results for the DH catalysts. In DH-1 catalyst which the Pt content is 0.1 wt. %, there is one broad peak which starts at 300°C and ends at 600°C . The maximum of this peak is at around 500°C , with a very small shoulder at the temperature about 370°C .

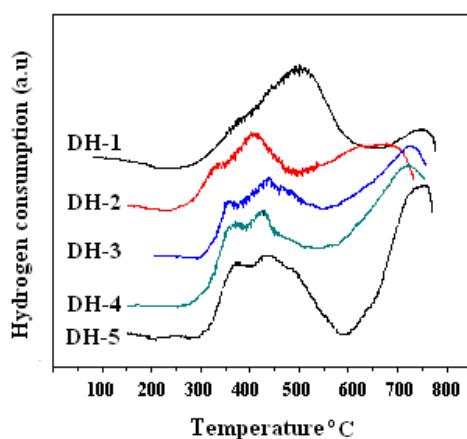


Fig. 8. The TPR profiles for catalysts DH-1 to DH-5

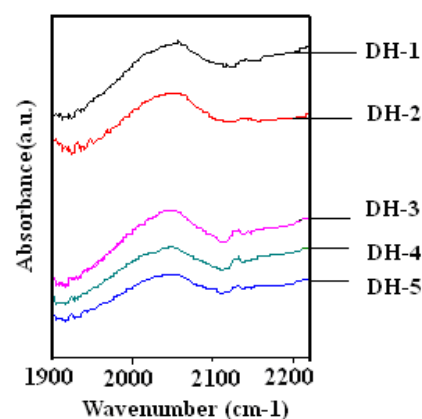


Fig. 11. FTIR spectra of adsorbed CO over prepared catalysts with different Pt loadings

In this sample, due to the great excess of Sn and In in comparison to the Pt content, major amount of Sn and In oxides are separated from Pt and need higher temperatures to be reduced. With increasing the Pt content of sample DH-2, two peaks are appeared at the temperature ranges between 270 – 470°C . The first peak would correspond to the reduction of platinum species in high interaction with the support, generating a surface complex which has

a maximum at 337°C [16, 25]. The second peak has a maximum at 408°C, which in comparison to the DH-1 sample, the second peak in DH-2 sample shifts to the lower temperatures with a reduction in the broadness of its peaks. These results indicate a few features including the reduction of a part of the oxides by Pt atoms, and a good interaction between the elements with probable alloy formation. These results also indicate that platinum facilitates the reduction of oxides in this catalyst. With increasing the Pt content in samples DH-3 to DH-5, the first peak becomes stronger and the maximum of the two peaks come closer. The TPR results for all the catalysts showed a reduction peak centered around 700°C, which is related to the some portions of the oxides might be strongly bonded among themselves or with the support [25].

3.2.3 Transmission electron microscopy (TEM)

Micrographs of transmission electron microscopy of DH-5 catalyst are shown in Figure 9. The dark parts in Figure 9 are believed to be metal clusters. The nanocrystalline gamma alumina support can be seen in the lighter areas. TEM results show a narrow distribution of metallic particle sizes, with a mean particle size of 2.6 nm for the prepared catalyst.

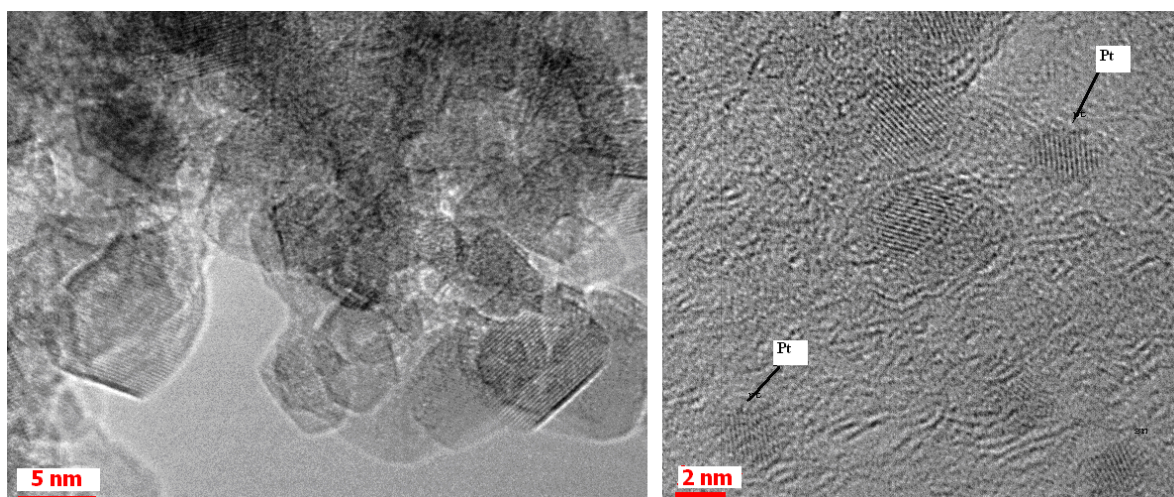


Fig. 9. Transmission electron micrographs of DH-5 catalyst

In high resolution micrograph, the Pt nanoparticles can be observed as it was shown for the samples DH-2 and DH-5 in Figure 10. As it can be seen platinum particle size increases with increasing the platinum concentration in all the catalysts. Smaller particle sizes show better dispersion and consequently better activity.

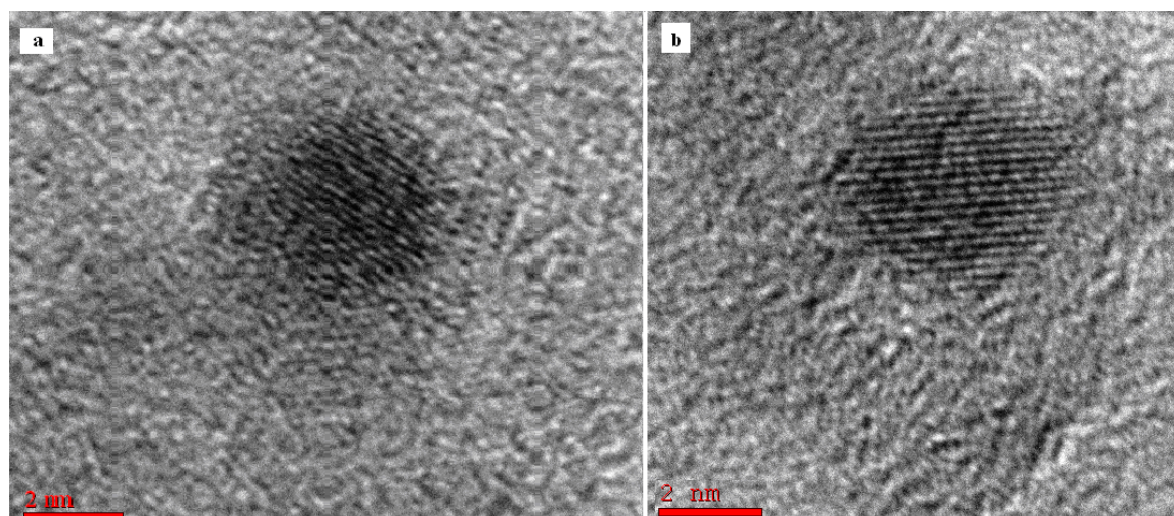


Fig. 10. High-resolution transmission electron microscopy images: (a) DH-2, (b) DH-5

3.2.4 CO chemisorption

Figure 11 represents the IR spectra of CO adsorbed (without further evacuation) at 25°C on the different Pt catalysts. In Figure 11 the bands which correspond to the linear form of CO adsorption on Pt, are shown. In the samples DH-1 and DH-2 the maximum of the peak related to Pt-CO linear adsorption slightly shifted to the higher frequencies in comparison to the other samples prepared (2066 cm⁻¹) [6, 26]. The other three samples have similar behavior and show a band at about 2063 cm⁻¹. Shifting the Pt-CO band to the lower wave numbers is an effect of decreasing in CO coverage. The integrated area of the IR band corresponding to the linear Pt-CO band decreases from the samples DH-1 to DH-5 as it can be seen in Table 4. Decreases in the CO chemisorptions capacity can be related to the decreases in the platinum dispersion from the catalysts DH-1 to DH-5.

Tab. 4. Integrated areas of the bands corresponding to the linear chemisorptions of CO on Pt sites

Catalyst	$I_{\text{CO-Pt}}$ (a.u. cm ⁻¹)
DH-1	4.27
DH-2	4.08
DH-3	3.91
DH-4	3.78
DH-5	3.45

4. Catalytic activity

The catalytic behavior has been studied using higher normal paraffins (C₁₀-C₁₅) as the feed. A summary of the catalytic behavior is presented in Table 5. The catalytic results also compared with a reference commercial IFP Company catalyst (DP-805). This catalyst contains 0.4 wt.% of platinum, 0.35 wt.% of tin, 0.2 wt.% of indium and 0.35 wt.% of lithium. The olefinic products which presented in Table 5 are mono olefins which are the desired products in higher normal paraffins dehydrogenation.

As it was expected, a temperature increase from 460 to 490°C, would cause the total conversion to increase and slightly decrease in selectivity to mono olefins.

In the samples DH-1 and DH-2 with an increase in the platinum contents the total conversion increases. However, in the samples DH-3, DH-4 and DH-5 with an increase in the platinum loading the activity of catalysts decreases. It can be concluded, it is not required to use large quantities of platinum to catalyze the reaction because of high dispersion of active phase on the synthesized nanocrystalline gamma alumina support.

Comparing the catalytic results of the samples prepared with the commercial catalyst (DP-805) which were tested at the same conditions showed the good performances of the catalysts prepared. The obtained results showed higher selectivity for all the prepared catalysts in comparison to the commercial catalyst which indicates the excellent performances of the catalysts prepared. In Figure 12, the catalytic results of the samples DH-2 and DP-805 are presented after 36 h on stream.

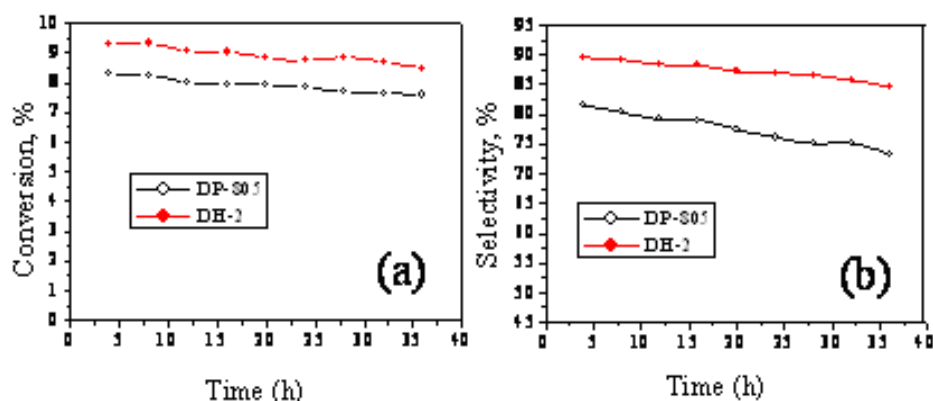


Fig. 12. (a) Conversion and (b) selectivity for catalysts DH-2 and DP-805 at 460°C during 36 h on stream

The temperature was fixed at 460 °C and the other test conditions kept unchanged except the H₂/HC molar ratio which is equal one. As the main function of hydrogen is decreasing the coke formation and consequently increasing the stability of the catalyst, it is decreased to investigate the catalytic activity under severe conditions. The results clearly indicate the higher conversion and higher mono olefins selectivity in the DH-2 catalyst. The loss of olefins selectivity in DP-805 catalyst is due to the secondary dehydrogenation to diene and then to aromatics and parallel formation of light paraffins. The decreases in the selectivity of mono olefins after 36 h were 11.8 and 5.1 % in commercial (DP-805) and DH-2 catalysts, respectively. These results show higher stability of the catalyst DH-2 in comparison to the commercial catalyst.

Table 5. The catalytic testing results of the prepared catalysts and the commercial catalyst in the dehydrogenation reaction of higher normal paraffins (C10-C15) at three different temperatures

Catalyst #	Temp. (°C)	Total conversion (%)	Olefins %	Selectivity (%)
DH-1	460	10.05	8.98	89.37
	475	12.83	11.22	87.47
	490	19.74	17.05	86.35
DH-2	460	10.40	9.31	89.44
	475	13.55	11.86	87.54
	490	19.96	17.24	86.39
DH-3	460	10.23	9.16	89.57
	475	12.92	11.31	87.59
	490	18.39	15.89	86.46
DH-4	460	9.78	8.80	89.92
	475	12.47	10.93	87.68
	490	16.43	14.21	86.50
DH-5	460	8.70	7.86	90.41
	475	11.55	10.43	90.23
	490	15.46	13.89	89.87
DP-805	460	10.19	8.28	81.24
	475	12.92	10.19	78.84
	490	17.18	12.74	74.18

5. Conclusions

Different dehydrogenation catalysts with the changes in platinum loading with using a nanocrystalline gamma alumina support were prepared. The results revealed that the olefinic products decrease with increase in the Pt loading. All the catalysts prepared showed high selectivity to mono olefins in comparison to the commercial catalyst, which the selectivity changed very slightly with increasing the temperature. The relationship between selectivity and activity causes difficulties because one who is seeking improved selectivity must often accept smaller yields or more numerous recycle streams. Accordingly, the art could greatly benefit from a catalyst which did not exhibit this trade off between activity and selectivity. The results obtained indicate the higher conversion and selectivity of the catalyst DH-2 (0.2 wt% of Pt) in comparison to the commercial catalyst (0.4 wt% of Pt). The most important conclusion from this research is the good performances of the catalysts with low platinum contents with using the synthesized nanocrystalline gamma alumina support with high surface area.

Acknowledgements

The authors would like to thank the Research&Technology center of the petrochemical company in Iran for their financial support.

References

- [1] Bell, A.T.:Catalysis Looks to the Future, National Academy Press, Washington D.C, 1992.
- [2] Padmavathi, G, Chaudhuri, K.K., Rajeshwer, D., Rao, G.S., Krishnamurthy, K.R., Trivedi, P.C., Hathi,K.K., Subramanyam,N.: Chem. Eng. Sci. 2005, 60, 4119.
- [3] He, S., Sun, C., Bai, Z., Dai, X., Wang, B.: Appl. Catal., A 2009, 356, 88.
- [4] Miguel, S.R., Castro , A.A., Scelza, O.A.:Catal. Lett. 1995, 32, 281.
- [5] Pieck, C.L., Vera, C.R., Querini, C.A., Parera, J.M.: Appl. Catal., A 2005, 278, 173.
- [6] Arteaga, G.J., Anderson, J.A., Rochester, C.H.: Catal. Lett. 1999, 58, 89.
- [7] He, S., Sun, C., Bai, Z., Dai, X., Wang, B.: Chem. Eng. J. 2008, 141, 284.
- [8] Bhasin, M.M., Mccain, J.H., Vora, B., Imai, T., Pujado, P.R.:Appl. Catal., A 2001, 221, 397.
- [9] Dongara, R., Basrur, A.G., Gokak, D.T., Gokak, K.V., Rao, V.,Krishnamurthy , K.R., Bhardwaj, I.S.: US Patent 5677260 , 1997.
- [10] Wilhelm, F.C.: US Patent 3998900 ,1993.
- [11] Passos, F.B., Andera, D.A.G., Schmal, M.: Catal. Today 2000, 57, 283.
- [12] Castro, A.A.: Catal. Lett. 1993, 22 , 123.
- [13] Sanfilippo, D., Miracca, I.: Catal. Today 2006,111,133.
- [14] Passos, F.B., Andera, D.A.G., Schmal, M.: J. Catal. 1998, 178, 478.
- [15] Tamotsu, I., Chi-Wen, H.: US Patent 4486547, 1984.
- [16] Carnevillier, C., Epron, F., Marecot, P.:Appl. Catal., A 2004, 275, 25.
- [17] G.J. Siri, J.M. Ramallo-Lopez, M.L. Casella, J.L. G. Fierro, F.G. Requejo, O.A. Ferretti, Appl. Catal., A 2005, 278 , 239.
- [18] Yoldas, B.E.: Am. Ceram. Soc. Bull. 1975, 54, 289.
- [19] Farias, R.F., Arnold, U., Martinez, L., Schuchardt, U., Jannini, M.J.D.M., Airoidi, C.: J. Phys. Chem. Solids 2003, 64, 2385.
- [20] Zhang, Z., Hicks, R.W., Pauly, T.R., Pinnavaia, T.J.:J. Am. Chem. Soc. 2002, 124, 1592.
- [21] Akia, M., Alavi, S.M., Rezaei, M., Zi-Feng, Y.: Microporous Mesoporous Mater. 2009, 122, 72.
- [22] Akia, M., Alavi, S.M., Rezaei, M.,Zi-Feng, Y.:J. Porous Mater. 2010, 17, 75.
- [23] Dilsiz, N., Akoval, G.: Mater. Sci. Eng. 2002, 332, 91.
- [24] Leofantia, G., Padovan, M., Tozzola, G., Venturelli, B.:Catal. Today 1998, 41, 207.
- [25] Carvalho, L.S., Reyes, P., Pecchi, G., Figoli, N., Pieck, C.L., Range, M.D.C.: Ind. Eng. Chem. Res. 2001, 40, 5557.
- [26] Merlen, E., Beccat, P., Bertolini, J.C., Delichere, P., Zanier, N., Didillon,B.: J. Catal. 1996, 163, 294.